

## Evaluating the Effect of 3D Printed Polycaprolactone-Boric Acid Scaffold on Proliferation and Bone Differentiation of Human Bone Marrow Mesenchymal Stem Cells

Milad Salemian<sup>1</sup> | Hanieh Jalali<sup>1,\*</sup> | Mohammad Nabiuni<sup>2</sup> | Homa Mohseni-Kouchesfehani<sup>1</sup>

<sup>1</sup>Department of Animal Biology, Faculty of Biological Sciences, Kharazmi University, Tehran, Iran

<sup>2</sup>Department of Cell and Molecular Biology, Faculty of Biological Sciences, Kharazmi University, Tehran, Iran

\*Corresponding Author E-mail: [jalali@khu.ac.ir](mailto:jalali@khu.ac.ir)

Submitted: 2024-02-01, Revised: 2024-03-16, Accepted: 2024-04-07

### Abstract

**Background:** Biocompatible implants are a suitable option in the reconstruction and repair of damaged bone and can be considered instead of bone grafting. However, the materials used to produce such substitutes may not have sufficient bioactivity in the body. Boric acid (BA) is a weak acid of boron with water solubility, semi-conductivity, and anti-inflammatory properties. It also stimulates bone formation in the body. The aim of this study was to produce a bone substitute composed of polycaprolactone (PCL) and BA using a 3D-printer and analyse its effect on the proliferation and bone differentiation of human bone marrow mesenchymal stem cells (hBMSCs).

**Methods:** PCL scaffolds containing different concentrations of BA were produced using a 3D printer and were characterized with scanning electron microscopy (SEM), Fourier transform infrared (FTIR) spectroscopy, and inductively coupled plasma mass spectrometry (ICP-MS). In addition, the proliferation and bone differentiation of human bone marrow mesenchymal stem cells (hBMSCs) on the PCL-BA scaffolds were evaluated using MTT assay, alizarin red staining, and alkaline phosphatase (ALP) measurement.

**Results:** BA was gradually released from the 3D scaffolds and PCL-BA scaffolds have a suitable three-dimensional structure for cell attachment and proliferation. According to the MTT results, PCL-BA scaffolds did not cause any toxicity to hBMSCs. Although PCL-BA scaffolds had significant osteoinduction potential, scaffold containing lower concentrations of BA had a better effect on osteogenesis.

**Conclusion:** BA incorporation enhanced the bioactivity of PCL scaffolds; however, the BA concentration was a determining factor in the direction of bone differentiation of hBMSCs.

**Keywords:** Tissue engineering, Bone, Boric acid, Three-dimensional printing, Polycaprolactone.

## Introduction

Although bone tissue has an inherent ability to self-heal, factors such as severe fractures, infection, and underlying diseases can delay or disrupt its repair [1]. Bone grafting is the most common method for treating severe bone injuries, but it has limitations such as low bone density in the donor and the risk of infection [2]. Because of the urgent need to develop alternative treatments that can achieve similar results to autografts and allografts, the bone tissue engineering has emerged and made rapid progress in recent decades [3]. The goal of bone tissue engineering is to induce the healing and regeneration of new tissue by leveraging the synergy between cells, signals, and scaffolds [4]. To obtain this goal, a biological material can be produced as a temporary matrix that provides a specific environment and architecture for the growth and differentiation of osteoblasts and provides sufficient support for the formation of bone tissue [5]. This temporary matrix called a scaffold, must have mechanical properties such as compatibility with bone tissue, biocompatibility, and osteoinductive potential [6]. To produce scaffolds suitable for tissue engineering applications, properties such as biological requirements, structural features, materials composition, and manufacturing processes can be improved or modified [7]. Various methods are used for producing scaffolds, such as phase separation, freeze-drying, solvent casting, and electrospinning; however, these methods have limitations in terms of control over scaffold structure [8]. The three-dimensional (3D) printers allow precise adjustment of the size, shape, cross-links, branching, geometry, and direction of pores within a scaffold, thereby increasing control over its mechanical properties, biological effects, and degradation kinetics [9]. Scaffolds

produced using 3D printers can also be of interest in personalized medicine, in which scaffolds can be made to an anatomical shape [10].

Polymers are widely employed in the production of 3D bone scaffolds due to their suitable mechanical properties, moldability, high thermal resistance, and non-toxicity [11]. However, they have limitations for bone tissue engineering due to their low bioactivity and high hydrophobicity and are therefore often combined with natural polymers or metal elements [12]. Polycaprolactone (PCL) is one of the most common materials used in the production of tissue engineering scaffolds. PCL is an FDA-approved linear polyester with good biocompatibility, slow degradation rate, low melting point, less acidic degradation products compared to other polyesters, and has the potential for drug delivery applications [13]. Although the mechanical properties of pure PCL, including high flexibility and elongation, make it a desirable option for preparing bone scaffolds, pure PCL has no osteogenic potential to induce bone regeneration, and also does not provide a favorable environment for cell attachment and growth due to its very high hydrophobicity [14]. Therefore, to address these limitations, researchers combine PCL with natural polymers such as collagen, gelatin, chitosan, minerals, or metal elements to enhance the properties of this scaffold for bone healing [15].

Boron (B) Q3 is a trace element with semiconducting properties absorbed by the digestive system from drinking water and plant foods and is often present in plasma as boric acid (BA) [16]. B is involved in the regulation of steroid hormones and prevents calcium excretion and bone demineralization [17]. It has also been shown that boron supplementation in postmenopausal women reduces urinary excretion of calcium and magnesium, as well as increases serum levels of estradiol and

calcium absorption [18]. Using MC3T3-E1 (a mouse calvarial osteoblastic cell line), the B effects on cell proliferation, mineralization, and expression of mRNA of genes related to mineralization were investigated, showing that the use of boron increased mineral nodule formation and expression of mRNA of type 1 collagen, osteopontin, bone sialoprotein, osteocalcin, and Runt-related transcription factor (Runx) [19]. BA, also known as orthoboric acid, is a weak acid of boron with antimicrobial and anti-inflammatory effects [20]. BA prevents osteoclast activity and inhibited the damage to bone caused by lipopolysaccharides [21]. In cases where inflammation occurs in bone, Receptor activator of nuclear factor kappa-B ligand (RANKL) is expressed by immune cells such as T lymphocytes at the inflammatory site and its binding to the receptor on the surface of pre-osteoclasts stimulates their differentiation into mature osteoclasts, resulting in bone resorption. A study on a model of alveolar bone injury in rats showed that feeding the injured animals with BA led to reduced RANKL expression periodontal inflammation and alveolar bone loss [22]. Studies have further shown that BA has osteoinductive properties and can be used to enhance the properties of scaffolds for bone tissue engineering purposes; for example, the combination of the BA-containing nanoparticles' combination with a chitosan scaffold prepared by the freeze-drying method resulted in increased bone differentiation in the MC3T3-E1 cell line [23].

Although BA is a viable option for integration with non-bioactive polymers such as PCL due to its water solubility, semi-conductivity, and anti-inflammatory properties, some studies have indicated some toxic effects [24]. Therefore, it is necessary to analyze the precise effect of different concentrations of BA to select a suitable combination of BA and PCL to

produce scaffolds with the highest bone-forming effect and prevent its adverse effects. In the present study, we prepared PCL scaffolds containing different concentrations of BA using a 3D printer and determined their effects on the proliferation and bone differentiation of human bone marrow mesenchymal stem cells (hBMSCs).

## Materials and Methods

### *Fabrication of Three-Dimensional Scaffolds Containing Boric Acid*

To prepare the scaffolds, 1-6 mM BA (Merck, Germany) solutions were mixed with 50 mg of PCL (Sigma-Aldrich, U.S.A), and then dissolved in chloroform (Merck, Germany). The solution was then placed on a shaker for 24 hours. The resulting BA-containing PCL was then precipitated and used to print a 3D scaffold (3DPL Bioprinters, jp4, Iran). The printing parameters were 60 mm/min, 3.38 bar, and 75 °C. PCL without any additives was applied as the control group.

### *Preparation and Culture of Bone Marrow Mesenchymal Stem Cells*

hBMSCs were obtained from Royan Institute, Iran, under contract number 054/1400. DMEM low glucose (Gibco, UK) medium containing 10% FBS (Gibco, UK) and 1% antibiotic was applied to culture the cells. The cells were placed in an incubator (Binder, Germany) with 5% CO<sub>2</sub> and 37 °C.

### *Determining the Rate of BA Release*

The release rate of BA from 3D printed discs was measured by inductively coupled plasma mass spectrometry (ICP-MS) over days 1, 3, and 7. To do this, 3D-PCL discs containing BA were placed in 5 mL phosphate-buffered saline (PBS) and incubated at 37 °C. After the specified period of time, the amount of BA released

from the disc into the upper environment was measured by an ICP-MS device (Agilent, U.S.A.).

#### *Mass Reduction Test for Scaffolds*

To study the degradation rate and mass loss of the scaffold, the discs were initially weighed and then placed in 5 mL PBS in an incubator at 37 °C. On days 3, 7, 10, and 14, the discs were removed from the container and weighed after complete drying. At the end of the experiment, mass loss was calculated using the following equation:

$$\% \text{ mass loss} = \frac{m_0 - m_t}{m_0} \times 100$$

Where,  $m_0$  and  $m_t$  are the mass of the samples before immersion in water and the mass of the dry samples at time  $t$  after immersion in water, respectively.

#### *Fourier Transform Infrared Spectroscopy (FTIR) Study of Samples*

To investigate the surface chemistry properties of the prepared scaffold, FTIR was applied using a 510A-WQF/Rayleigh analyzer made in China, in the range of wave number 4000-400  $\text{cm}^{-1}$  with resolution 4  $\text{cm}^{-1}$ .

#### *Scanning Electron Microscopy Imaging*

Scanning electron microscopy (SEM) was applied to investigate the morphology of the 3D-printed scaffolds. In this regard, the disks were fixed in a 4% solution of glutaraldehyde (Merck, Germany) for 1.5 hours. The samples were dehydrated with increasing concentrations of ethanol and finally dried and coated with gold before being imaged with a Philips XL30 SEM microscope manufactured by Philips in the Netherlands.

#### *Measuring the Cytotoxicity of Scaffolds*

To determine the cytotoxicity of 3D-printed scaffolds containing BA, the disks surface was initially modified with oxygen gas plasma for 3 minutes at a pressure of 6.0 millibars and a power of 60% to increase the wettability of the surface. Subsequently, the disks were sterilized and positioned at the bottom of each well in a 96-well plate, and then 30,000 cells were seeded on each disk and the 3-(4,5-dimethylthiazol-2-yl)-2,5-diphenyltetrazolium bromide (MTT) test was conducted after 3 and 7 days. For this purpose, the culture medium was first removed and the wells of the plate were gently washed with PBS (Gibco, UK), and then 10  $\mu\text{l}$  of a solution of MTT (5 mg/ml) (Lifebiolab, Germany) was added to each well in the dark, and the plate was incubated for 4 hours. After the end of the treatment time, media were discarded and 100  $\mu\text{l}$  of Dimethyl sulfoxide (DMSO) (Merck, Germany) were added to each well and pipetted, and then the optical absorption at a wavelength of 450 nanometers was transferred. The percentage of live cells was calculated according to the following equation:

$$\% \text{ viability} = \frac{\text{OD}_{\text{Test}}}{\text{OD}_{\text{Control}}} \times 100$$

#### *Bone Differentiation of hBMSCs Cells on the 3D- Printed Scaffolds*

The osteogenic potential of the produced scaffolds was determined using Alizarin Red S staining and alkaline phosphatase content measurement. To do this, the cells were first cultured on the surface of the scaffolds, and then incubated for 14 and 21 days in a bone differentiation medium containing DMEM medium enriched with 50 mg/ml 2-phosphate ascorbic acid, 10 nM/mL dexamethasone, and 10 mM beta glycerol phosphate (all from Sigma, USA) [25]. Afterwards, the culture medium was

removed from the cells and the cells were washed with PBS, and then the cells were fixed with 4% glutaraldehyde for 30 minutes and washed again with PBS. Eventually, 1% Alizarin Red S (Merck, Germany) was added and incubated at room temperature for 30 minutes. Finally, PBS washing was performed to remove excess dye and mineral deposition was visualized by light microscope. To measure the alkaline phosphatase content, 14 days after culturing the cells in the bone differentiation medium, the culture medium was removed from the cells and the cells were washed with PBS. After that, 200  $\mu$ L of 0.1% Triton X-100 was added to each well and incubated on a shaker for 20 minutes, and then the alkaline phosphatase kit from Biorex Fars, Iran, was applied and read at a wavelength of 405 nanometers using a 350UV-Vis Camspec M spectrophotometer.

### Statistical Analysis

All experiments were repeated at least three times and p-value < 0.05 was considered significant. To analyze the results and draw graphs, GraphPad Prism software and one-way analysis of variance (ANOVA) were used.

## Results

### BA Gradual Release from 3D-Printed Scaffolds

The results of ICP-MS analysis showed that BA was gradually released from the scaffolds so that the amount of BA released in the environment increased with time of immersion in PBS. Also, the results confirmed that scaffolds with higher amount of BA had more rate of BA release during the time (Figure 1).

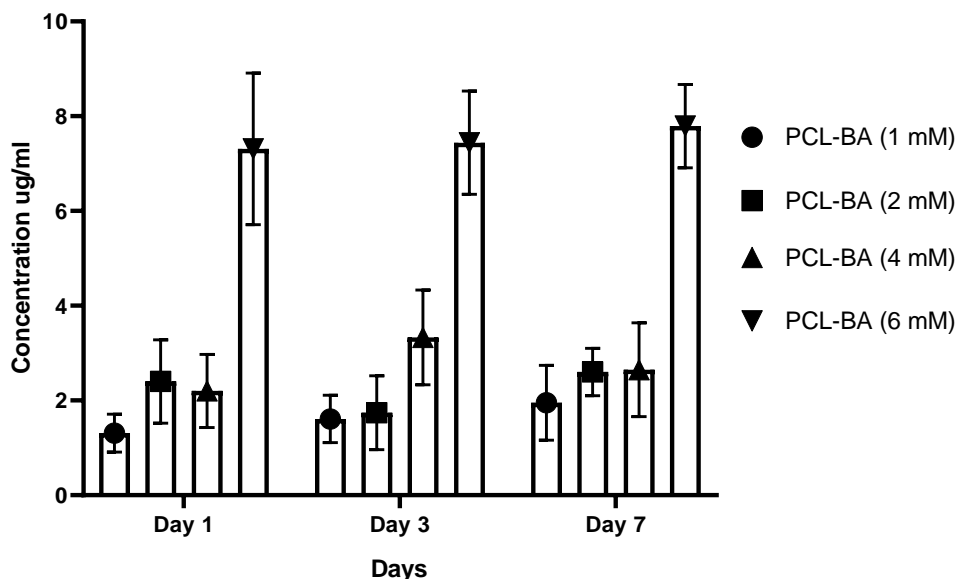


**Figure 1** Concentration of boric acid (BA) released from scaffolds based on the ICP-MS assay. Data are presenting Mean  $\pm$  S.D

### Degradation Rate of BA-PCL 3D-Printed Scaffolds

The results of the mass loss test revealed that the PCL scaffold had less

degradation rate compared to the scaffolds containing BA. Moreover, the results showed an increase in mass loss with increasing boric acid concentration in the scaffold. This implies that the

degradation of the PCL scaffolds increased with an increase in BA concentration (Figure 2).

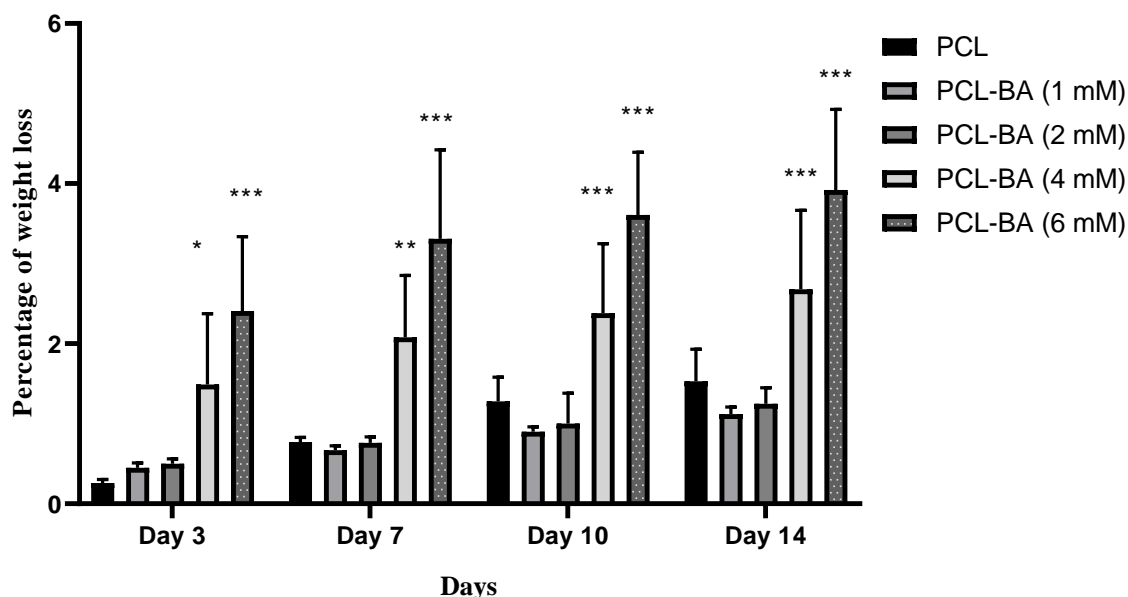


**Figure 2** The mass loss rate of polycaprolactone (PCL) scaffold containing different concentrations of boric acid (BA) compared to PCL scaffold. Data are presenting Mean  $\pm$  S.D. \*:  $p < 0.05$ , \*\*:  $p < 0.01$ , and \*\*\*:  $p < 0.001$

### FTIR Spectroscopy Results

In this study, FTIR spectroscopy was used to detect possible interactions between BA particles and PCL. PCL (Figure 3A) has three characteristic peaks at wave numbers of approximately 1159, 1719, and 2863  $\text{cm}^{-1}$ , which respectively indicate the stretching vibrations of the C-C, C=O, and  $\text{CH}_2$  bonds. The three characteristic peaks of PCL were also observed in the 3D PCL scaffold containing BA (Figure 3B). Therefore, no difference was observed between the spectrum of pure PCL and the composite PCL containing BA.

### Analyzing the Structure of 3D-Printed Scaffold by SEM Microscopy

The results of SEM imaging of 3D-printed scaffolds demonstrated uniform

and homogeneous porosity, so that, the diameter of each longitudinal fiber was  $426 \pm 37 \mu\text{m}$ , while the diameter of each transverse fiber was  $413 \pm 29 \mu\text{m}$  (Figure 4).

### Cytocompatibility of 3D-Printed PCL-BA Scaffolds

Results obtained from MTT assay demonstrated that in the third and seventh days after culture, the percentage of live cells on the 4 and 6 mM BA-containing scaffolds was significantly different from the PCL scaffold at the  $p < 0.05$  level. The results of the analysis among different groups showed that cell growth had a direct relationship with the concentration of BA, such that cell growth increased with increasing BA concentration in the disks (Figure 5).

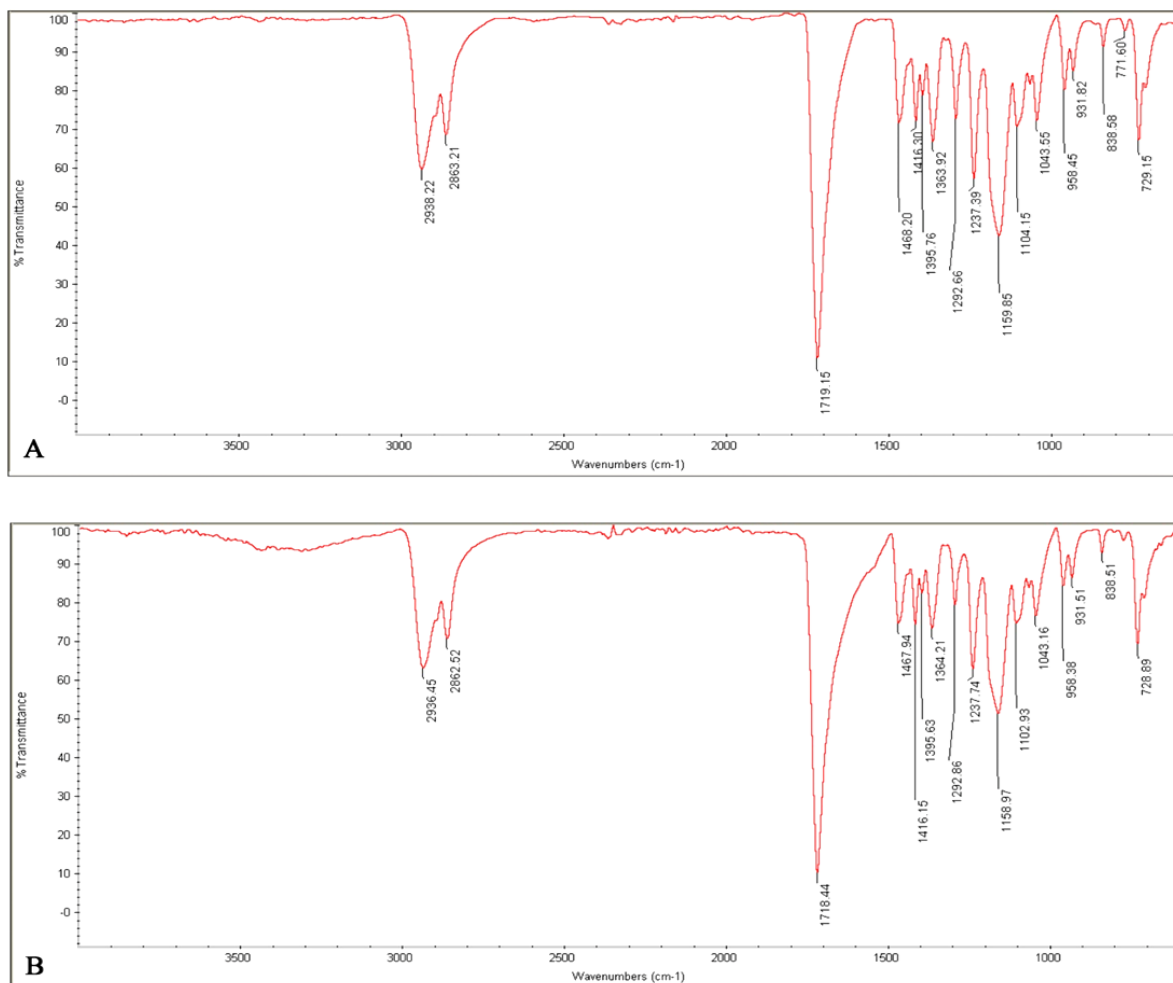


**Figure 3** FTIR absorption spectra of A: polycaprolactone scaffold, and B: polycaprolactone group containing boric acid

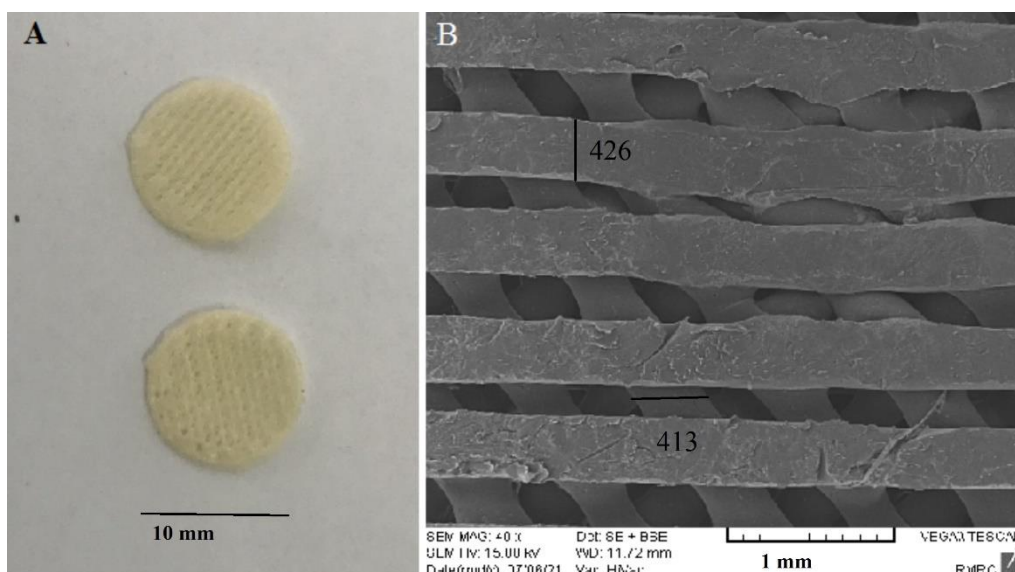


**Figure 4** Structure of 3D-printed disks. A: the appearance of 3D-printed disks and B: SEM imaging of a 3D printed disc showing the arrangement of fibers and their diameter

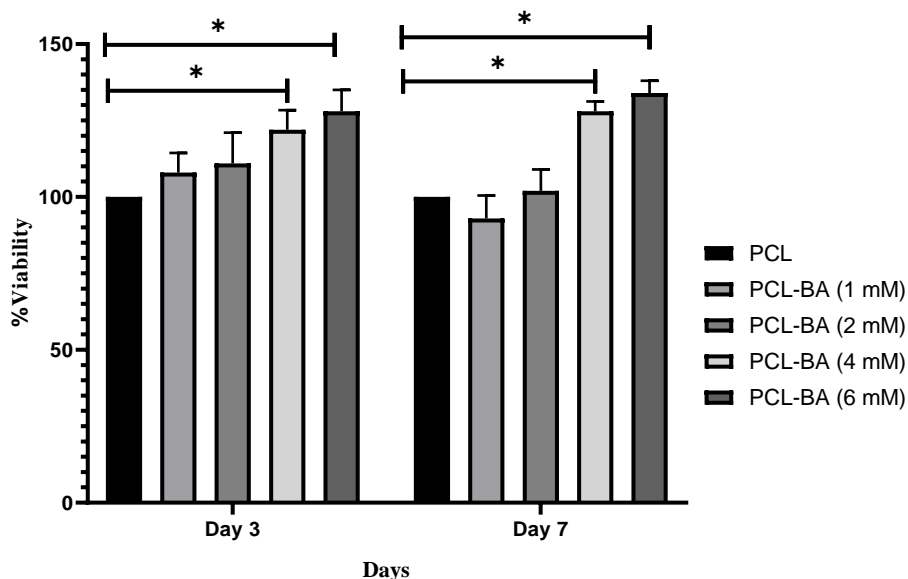


**Figure 5** Evaluating the proliferation of hBMSCs on the 3D-printed scaffolds containing different concentration of boric acid (BA) during the three and seven days. \*: significant difference between the treatments at a level of less than 0.05 compared to the control group, n = 3, and Mean ± S.D

*Osteogenesis in PCL Scaffolds Containing BA*

The results of the Alizarin Red staining indicated that the group containing 6 mM had less extracellular calcium formation than the control group. However, when cells were differentiated on the scaffold

containing 2 mM, more extracellular calcium was formed. Comparison of the results of the alkaline phosphatase content also showed that the ALP in the PCL containing 6 mM boric acid group was lower than the ALP in PCL containing 2 mM boric acid (Figure 6).

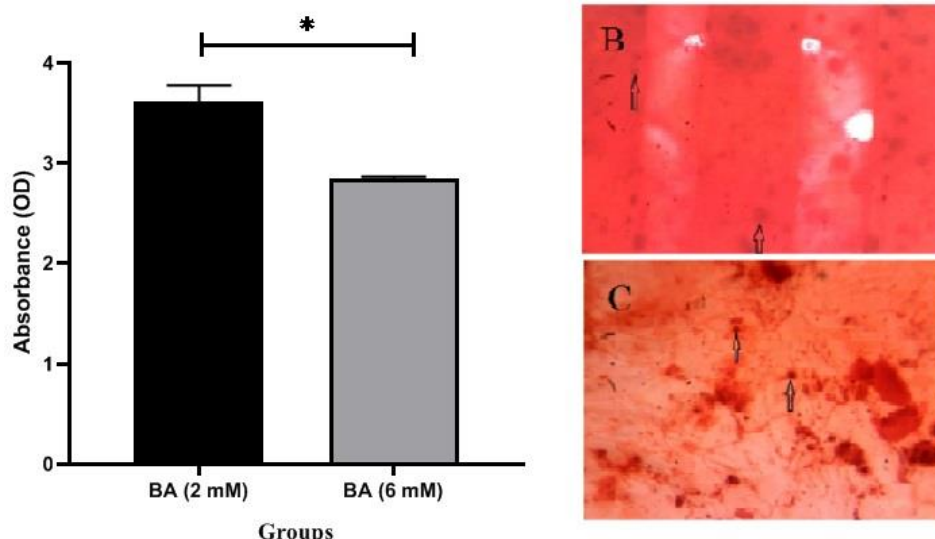


**Figure 6** Evaluation the osteogenic differentiation of hBMSCs on the 3D-printed scaffolds containing different concentration of boric acid (BA) during the three and seven days. A: Comparison the alkaline phosphatase activity, B and C: presence of mineralized matrix on the scaffolds containing 6mM and 2 mM. BA\*: Significant difference between the treatments at a level of less than 0.05 compared to the control group, n = 3, and Mean ± S.D



## Discussion

Several studies have shown that trace elements have an impact on bone metabolism and tissue properties, which either act by regulating macro mineral metabolism, or act by influencing the proliferation or activity of osteoblasts and osteoclasts, or by becoming part of the bone mineral matrix [26]. In the present study, B was added to PCL in the form of BA at various concentrations. The degradation, biocompatibility, and bone-forming ability of the scaffolds were then evaluated. The results indicated that BA had a gradual and slow release from the synthesized scaffolds. This controlled release mechanism ensures a long-term supply of this substance at the damaged site, and also prevent the toxic effects of high doses. The amount of BA released substance from the disks on the 7th day was 2-7  $\mu\text{g/ml}$  that based on previous reports; this range of BA does not exhibit cellular toxicity [27,28]. Combining the BA with PCL prevented the explosive release of the substance and toxicity to cells, and proved that PCL can be a viable option in the controlled delivery of BA. PCL has long been of interest in the field of drug delivery due to its slow degradation that allows for controlled drug release [29]. Micro pores in scaffolds affect cell penetration and cell distribution, and more importantly, they can facilitate the transport of gases and nutrients to the deeper layer of the scaffolds and thus maintain cell survival. Moreover, adjusting the size of micro pores can regulate the release behavior of drugs/biological molecules/loaded factors in the scaffold matrix or absorbed/bound/conjugated on the scaffold surface [30]. In the current study, 3D-pinted scaffolds had uniform porosity that helped to maintain the shape and strength of the scaffold.

To produce a composite scaffold, it is crucial to ensure that the combined

material with PCL does not reduce biocompatibility or cause toxicity. BMSCs are a key component in tissue engineering, as they can differentiate into bone, cartilage, along with that they have low immunogenicity, and demonstrate immune-modulatory capabilities [31]. BMSCs are essential components in the process of forming new bone; from a therapeutic standpoint, BMSCs are relatively easy to obtain and the risk of tumors after their implantation is low [32]. In response to injury signals, BMSCs can potentially move from their location to the peripheral circulation and cross the vascular wall to reach target tissues [33]. The BMSCs effectiveness in cell therapy relies on their ability to home and adhere to the site of injury for a long period of time [34]. In this study, we investigated the toxicity of the produced scaffolds on BMSCs that revealed no toxic effect of BA-PCL scaffolds on the hBMSCs. Our findings align with a study by Akdere *et al.* in 2019 [35], who investigated the effect of concentrations of 1, 10, and 20  $\mu\text{g/ml}$  of B on the growth and survival of adipose tissue mesenchymal stem cells, and their results showed that treatment of cells with these boron concentrations causes cell growth and increased cell survival compared to the control group. Previously, Wu *et al.* also showed that the integration of B with bioactive glass scaffolds increased the growth of osteoblast cells [36].

The improvement of bone formation capacity of stem cells after treatment with BA has been confirmed by various *in vivo* and *in vitro* studies, which suggests that growth is highly dependent on the dosage of BA [37]. Our results indicated that although all the concentrations created in the environment had a positive effect on the BMSCs growth, in terms of bone differentiation, scaffolds containing high concentrations of BA had less stimulating effect and the highest bone differentiation occurred in the presence of PCL discs

containing low concentration of BA. These results are consistent with a study conducted by Movahedi Najafabadi *et al.* in 2016, which demonstrated that a concentration of 6 µg/ml of B had no significant effect on increasing bone differentiation of bone marrow mesenchymal stem cells, and a lower concentration of B had a significant effect on increasing bone differentiation of these cells [38].

Our results are also in agreement with the results of Li *et al.*, who measured the effect of boron nitride nanotubes on bone differentiation and alkaline phosphatase activity of mesenchymal stem cells; according to their findings, low concentration of boron nitride also led to a significant increase in alkaline phosphatase activity 14 days after differentiation, while high concentration did not affect bone differentiation and alkaline phosphatase activity compared to control cells [39]. The dose-dependent effect of BA on the differentiation of other cell types, including muscle cells, has also been established. Treatment of adipose-derived mesenchymal stem cells with concentrations of 5-2000 µg/ml of BA showed that although BA did not exhibit any toxic effects on the cells, lower doses of BA had a better effect on myogenic differentiation [40].

## Conclusion

This study demonstrated that PCL-BA 3D-printed scaffolds exhibited biocompatibility, posing no toxicity to hBMSCs. The boric acid concentration within the scaffolds played a pivotal role in their bioactivity. Scaffolds with higher boric acid stimulated growth of hBMSCs, while those with lower levels induced bone differentiation in hBMSCs. This finding can be considered in the fabrication of scaffolds with precise effect.

## Acknowledgments

The authors would like to thank the vice-chancellor research of Kharazmi University for its support.

## Funding

This study received no specific grant from any funding agency in the public, commercial, or not-for-profit sectors.

## Ethical statement

All ethical guidelines were followed during the study according to the ethical code number 990924105/616 approved by the Kharazmi University Ethics Committee.

## Declaration of Interests

The authors declare that there is no conflict of interest in this study.

## Authors' Contributions

Milad Salemian did experiments and data analyzing; Hanieh Jalali conducted conception, study designing, and article writing. All authors have read the manuscript and authorized the final version of the manuscript.

## ORCID

Milad Salemian

<https://orcid.org/0009-0001-9950-9987>

Hanieh Jalali

<https://orcid.org/0000-0002-8133-8729>

Mohammad Nabiuni

<https://orcid.org/0000-0001-7778-5406>

Homa Mohseni-Kouchesfehiani

<https://orcid.org/0000-0002-1234-1617>

## References

1. Gomez-Barrena E, Rosset P, Lozano D, Stanovici J, Ermthaller C, Gerbhard F. Bone fracture healing: cell therapy in delayed unions and nonunions, *Bone*;

- 2015; 70:93-101. [[Crossref](#)], [[Google scholar](#)], [[Publisher](#)]
2. Perez JR, Kouroupis D, Li DJ, Best TM, Kaplan L, Correa D. Tissue Engineering and Cell-Based Therapies for Fractures and Bone Defects, *Front Bioeng Biotechnol*; 2018; 6:105. [[Crossref](#)], [[Google scholar](#)], [[Publisher](#)]
3. Li JJ, Ebied M, Xu J, Zreiqat H. Current Approaches to Bone Tissue Engineering: The Interface between Biology and Engineering, *Adv Healthc Mater*; 2018; 7(6):e1701061. [[Crossref](#)], [[Google scholar](#)], [[Publisher](#)]
4. Huang R-L, Kobayashi E, Liu K, Li Q. Bone graft prefabrication following the in vivo bioreactor principle, *EBioMedicine*; 2016; 12:43-54. [[Crossref](#)], [[Google scholar](#)], [[Publisher](#)]
5. Bouet G, Marchat D, Cruel M, Malaval L, Vico L. In vitro three-dimensional bone tissue models: from cells to controlled and dynamic environment, *Tissue Engineering Part B: Reviews*, 2015; 21(1):133-56. [[Crossref](#)], [[Google scholar](#)], [[Publisher](#)]
6. Maurice N, Collins GR, Kieran Young, S. Pina, Rui L. Reis, J. Miguel Oliveira. Scaffold Fabrication Technologies and Structure/Function Properties in Bone Tissue Engineering, *Advanced Functional Materials*; 2021; 31(21). [[Crossref](#)], [[Google scholar](#)], [[Publisher](#)]
7. Roseti L, Parisi V, Petretta M, Cavallo C, Desando G, Bartolotti I, et al. Scaffolds for Bone Tissue Engineering: State of the art and new perspectives, *Materials Science and Engineering: C*, 2017; 78:1246-62. [[Crossref](#)], [[Google scholar](#)], [[Publisher](#)]
8. Peric Kacarevic Z, Rider P, Alkildani S, Retnasingh S, Pejakic M, Schnettler R, et al. An introduction to bone tissue engineering, *The International Journal of Artificial Organs*; 2020; 43(2):69-86. [[Crossref](#)], [[Google scholar](#)], [[Publisher](#)]
9. Feng Y, Zhu S, Mei D, Li J, Zhang J, Yang S, et al. Application of 3D Printing Technology in Bone Tissue Engineering: A Review, *Current Drug Delivery*; 2021; 18(7):847-61. [[Crossref](#)], [[Google scholar](#)], [[Publisher](#)]
10. Chia HN, Wu BM. Recent advances in 3D printing of biomaterials, *Journal of Biological Engineering*; 2015; 9:4. [[Crossref](#)], [[Google scholar](#)], [[Publisher](#)]
11. Nair LS, Laurencin CT. Polymers as biomaterials for tissue engineering and controlled drug delivery, *Advances in Biochemical Engineering/Biotechnology*, 2006; 102:47-90. [[Crossref](#)], [[Google scholar](#)], [[Publisher](#)]
12. Babilotte J, Guduric V, Le Nihouannen D, Naveau A, Fricain JC, Catros S. 3D printed polymer-mineral composite biomaterials for bone tissue engineering: Fabrication and characterization, *J Biomed Mater Res B Appl Biomater*; 2019; 107(8):2579-95. [[Crossref](#)], [[Google scholar](#)], [[Publisher](#)]
13. Guo W, Chen M, Wang Z, Tian Y, Zheng J, Gao S, et al. 3D-printed cell-free PCL-MECM scaffold with biomimetic micro-structure and micro-environment to enhance in situ meniscus regeneration, *Bioactive Materials*; 2021; 6(10):3620-33. [[Crossref](#)], [[Google scholar](#)], [[Publisher](#)]
14. Petretta M, Gambardella A, Boi M, Berni M, Cavallo C, Marchiori G, et al. Composite Scaffolds for Bone Tissue Regeneration Based on PCL and Mg-Containing Bioactive Glasses, *Biology (Basel)*; 2021; 10(5). [[Crossref](#)], [[Google scholar](#)], [[Publisher](#)]
15. Park SA, Lee H-J, Kim S-Y, Kim K-S, Jo D-W, Park S-Y. Three-dimensionally printed polycaprolactone/beta-tricalcium phosphate scaffold was more effective as an rhBMP-2 carrier for new bone formation than polycaprolactone alone, *Journal of Biomedical Materials Research Part A*; 2021; 109(6):840-8. [[Crossref](#)], [[Google scholar](#)], [[Publisher](#)]
16. Kose BZ-KaDA. Boric acid: a simple molecule of physiologic, therapeutic and prebiotic significance, *Pure and Applied Chemistry*; 2015; 87(2). [[Crossref](#)], [[Google scholar](#)], [[Publisher](#)]

17. Mohammad Reza Naghii MM, Ali Reza Asgari, Mehdi Hedayati, Maryam-Saddat Daneshpour. Comparative effects of daily and weekly boron supplementation on plasma steroid hormones and proinflammatory cytokines, *Journal of Trace Elements in Medicine and Biology*; 2011; 25(1):54-8. [[Crossref](#)], [[Google scholar](#)], [[Publisher](#)]
18. Pizzorno L. Nothing Boring About Boron, *Integrative Medicine (Encinitas)*; 2015; 14(4):35-48. [[Google scholar](#)], [[Publisher](#)]
19. Hakki SS, Bozkurt BS, Hakki EE. Boron regulates mineralized tissue-associated proteins in osteoblasts (MC3T3-E1), *Journal of Trace Elements in Medicine and Biology*; 2010; 24(4):243-50. [[Crossref](#)], [[Google scholar](#)], [[Publisher](#)]
20. Nazmus Shalehin AH, Hiroaki Takebe, Md Riasat Hasan, Kazuharu Irie. Boric acid inhibits alveolar bone loss in rat experimental periodontitis through diminished bone resorption and enhanced osteoblast formation, *Journal of Dental Sciences*; 2020; 15(4):437-44. [[Crossref](#)], [[Google scholar](#)], [[Publisher](#)]
21. Xu B, Dong F, Yang P, Wang Z, Yan M, Fang J, et al. Boric Acid Inhibits RANKL-Stimulated Osteoclastogenesis In Vitro and Attenuates LPS-Induced Bone Loss In Vivo, *Biological Trace Element Research*; 2023; 201(3):1388-97. [[Crossref](#)], [[Google scholar](#)], [[Publisher](#)]
22. Saglam M, Hatipoglu M, Koseoglu S, Esen HH, Kelebek S. Boric acid inhibits alveolar bone loss in rats by affecting RANKL and osteoprotegerin expression, *Journal of Periodontal Research*; 2014; 49(4):472-9. [[Crossref](#)], [[Google scholar](#)], [[Publisher](#)]
23. Menemşe Gümüşderelioğlu EÖT, Gökçe Kaynak Bayrak, Tuğrul Tolga Demirtaş, R. Seda Tıgılı Aydın, Sema S Hakki. Encapsulated boron as an osteoinductive agent for bone scaffolds, *Journal of Trace Elements in Medicine and Biology*; 2015; 31:120-8. [[Crossref](#)], [[Google scholar](#)], [[Publisher](#)]
24. Yalcin CO, Abudayyak M. Effects of boric acid on cell death and oxidative stress of mouse TM3 Leydig cells in vitro, *J Trace Elem Med Biol*; 2020; 61:126506. [[Crossref](#)], [[Google scholar](#)], [[Publisher](#)]
25. Force UPST. Vitamin D, Calcium, or Combined Supplementation for the Primary Prevention of Fractures in Community-Dwelling Adults: US Preventive Services Task Force Recommendation Statement, *JAMA*; 2018; 319(15):1592-9. [[Crossref](#)], [[Publisher](#)]
26. Ciosek Ż, Kot K, Kosik-Bogacka D, Łanocha-Arendarczyk N, Rotter I. The Effects of Calcium, Magnesium, Phosphorus, Fluoride, and Lead on Bone Tissue, *Biomolecules*; 2021; 11(4):506. [[Crossref](#)], [[Google scholar](#)], [[Publisher](#)]
27. Yilmaz Sarialtin S, Ustundag A, Mhlanga Chinheya R, Ipek S, Duydu Y. Cytotoxicity, genotoxicity, oxidative stress, apoptosis, and cell cycle arrest in human Sertoli cells exposed to boric acid, *Journal of Trace Elements in Medicine and Biology*; 2022; 70:126913. [[Crossref](#)], [[Google scholar](#)], [[Publisher](#)]
28. Giulia Paties Montagner SD, Simona Piaggi, Alfonso Pompella ORCID and Alessandro Corti \*ORCID. Redox Mechanisms Underlying the Cytostatic Effects of Boric Acid on Cancer Cells—An Issue Still Open *Antioxidants (Basel)*; 2023; 12(6). [[Crossref](#)], [[Google scholar](#)], [[Publisher](#)]
29. Ranjitsinh Pawar AP, Srishti Nagaraj, Harshad Kapare, Prabhanjan Giram, Ravindra Wavhale. Polycaprolactone and its derivatives for drug delivery, *Polymers for Advanced Technologies*; 2023; 34(10):3296-316. [[Crossref](#)], [[Google scholar](#)], [[Publisher](#)]
30. Marta Cavo a b SS. Scaffold microstructure effects on functional and mechanical performance: Integration of theoretical and experimental approaches for bone tissue engineering applications, *Materials Science and Engineering: C*;

- 2016; 68:872-9. [Crossref], [Google scholar], [Publisher]
31. Lu J, Shen X, Sun X, Yin H, Yang S, Lu C, et al. Increased recruitment of endogenous stem cells and chondrogenic differentiation by a composite scaffold containing bone marrow homing peptide for cartilage regeneration, *Theranostics*; 2018; 8(18):5039. [Crossref], [Google scholar], [Publisher]
32. Yang X, Yang J, Lei P, Wen T. LncRNA MALAT1 shuttled by bone marrow-derived mesenchymal stem cells-secreted exosomes alleviates osteoporosis through mediating microRNA-34c/SATB2 axis, *Aging (Albany NY)*; 2019; 11(20):8777. [Crossref], [Google scholar], [Publisher]
33. Funari A, Alimandi M, Pierelli L, Pino V, Gentileschi S, Sacchetti B. Human sinusoidal subendothelial cells regulate homing and invasion of circulating metastatic prostate cancer cells to bone marrow, *Cancers*; 2019; 11(6):763. [Crossref], [Google scholar], [Publisher]
34. Lin W, Xu L, Zwingenberger S, Gibon E, Goodman SB, Li G. Mesenchymal stem cells homing to improve bone healing, *Journal of Orthopaedic Translation*; 2017; 9:19-27. [Crossref], [Google scholar], [Publisher]
35. Akdere ÖE, Shikhaliyeva İ, Gümüşderelioğlu M. Boron mediated 2D and 3D cultures of adipose derived mesenchymal stem cells, *Cytotechnology*; 2019; 71(2):611-22. [Crossref], [Google scholar], [Publisher]
36. Wu C, Miron R, Sculean A, Kaskel S, Doert T, Schulze R, et al. Proliferation, differentiation and gene expression of osteoblasts in boron-containing associated with dexamethasone deliver from mesoporous bioactive glass scaffolds, *Biomaterials*; 2011; 32(29):7068-78. [Crossref], [Google scholar], [Publisher]
37. Marie-Hélène Thibault CC, Guillaume Vienneau, Jacques Robichaud, Delilah Brown, Ralf Bruening, Luc J. Martin, Yahia Djaoued. Assessing the potential of boronic acid/chitosan/bioglass composite materials for tissue engineering applications, *Materials Science and Engineering: C*; 2020; 110:1-8. [Crossref], [Google scholar], [Publisher]
38. Movahedi Najafabadi B-a-h, Abnosi MH. Boron Induces Early Matrix Mineralization via Calcium Deposition and Elevation of Alkaline Phosphatase Activity in Differentiated Rat Bone Marrow Mesenchymal Stem Cells, *Cell Journal (Yakhteh)*; 2016; 18(1):62-73. [Crossref], [Google scholar], [Publisher]
39. Li X, Wang X, Jiang X, Yamaguchi M, Ito A, Bando Y, et al. Boron nitride nanotube-enhanced osteogenic differentiation of mesenchymal stem cells, *Journal of Biomedical Materials Research Part B: Applied Biomaterials*; 2016; 104(2):323-9. [Crossref], [Google scholar], [Publisher]
40. Hüseyin Apdik AD, Selami Demirci, Safa Aydın, Fikretin Şahin. Dose-dependent Effect of Boric Acid on Myogenic Differentiation of Human Adipose-derived Stem Cells (hADSCs), *Biological Trace Element Research*; 2015; 165:123-30. [Crossref], [Google scholar], [Publisher]

**How to cite this article:**

M. Salemian, H. Jalali, M. Nabiuni, H. Mohseni-Kouchesfehiani. Evaluating the Effect of 3D Printed Polycaprolactone-Boric Acid Scaffold on Proliferation and Bone Differentiation of Human Bone Marrow Mesenchymal Stem Cells. *International Journal of Advanced Biological and Biomedical Research*, 2024, 12(3), 248-261.

DOI: <https://doi.org/10.48309/IJABBR.2024.2021433.1486>

Link: [https://www.ijabbr.com/article\\_712366.html](https://www.ijabbr.com/article_712366.html)

Copyright © 2024 by authors and SPC ([Sami Publishing Company](#)) + is an open access article distributed under the Creative Commons Attribution License (CC BY) license (<https://creativecommons.org/licenses/by/4.0/>), which permits unrestricted use, distribution, and reproduction in any medium, provided the original work is properly cited.